

Simple Model for the Variation of Superfluid Density with Zn Concentration in $\text{YBa}_2\text{Cu}_3\text{O}_{7-\delta}$

Jeng-Da Chai, Sergey V. Barabash, and D. Stroud*

Department of Physics, The Ohio State University, Columbus, Ohio 43210

(October 31, 2018)

Abstract

We describe a simple model for calculating the zero-temperature superfluid density of Zn-doped $\text{YBa}_2\text{Cu}_3\text{O}_{7-\delta}$ as a function of the fraction x of in-plane Cu atoms which are replaced by Zn. The basis of the calculation is a “Swiss cheese” picture of a single CuO_2 layer, in which a substitutional Zn impurity creates a normal region of area $\pi\xi_{ab}^2$ around it as originally suggested by Nachumi *et al.* Here ξ_{ab} is the zero-temperature in-plane coherence length at $x = 0$. We use this picture to calculate the variation of the in-plane superfluid density with x at temperature $T = 0$, using both a numerical approach and an analytical approximation. For $\delta = 0.37$, if we use the value $\xi_{ab} = 18.3 \text{ \AA}$, we find that the in-plane superfluid decreases with increasing x and vanishes near $x_c = 0.01$ in the analytical approximation, and near $x_c = 0.014$ in the numerical approach. x_c is quite sensitive to ξ_{ab} , whose value is not widely agreed upon. The model also predicts a peak in the real part of the conductivity, $\text{Re}\sigma_e(\omega, x)$, at concentrations $x \sim x_c$, and low frequencies, and a variation of critical current density with x of the form $J_c(x) \propto n_{S,e}(x)^{7/4}$ near percolation, where $n_{S,e}(x)$ is the in-plane superfluid density.

I. INTRODUCTION

In typical s-wave superconductors, nonmagnetic impurities are not pair-breaking, and therefore have little effect on either the transition temperature or the superfluid density [1]. By contrast, the substitution of a nonmagnetic impurity into a d-wave superconductor is expected to be pair-breaking, and, therefore, should have a significant effect on both. Since the CuO_2 -based high-temperature superconductors are believed to possess an order parameter with $d_{x^2-y^2}$ symmetry [2], such an effect should be observable in these materials. Indeed, the substitution of a nonmagnetic impurity such as Zn (or even an insulating impurity such

*Corresponding author: tel. (614)292-8140; fax (614)292-7557; email stroud@mps.ohio-state.edu

as He, introduced by ion implantation) in a high- T_c material such as $\text{YBa}_2\text{Cu}_3\text{O}_{7-\delta}$ is now well known to dramatically suppress the zero-temperature superfluid density [3–8] and also to have a significant, though lesser, effect on the critical temperature.

This striking behavior has provoked numerous theoretical studies of Zn impurities and other nonmagnetic disorder in the cuprate superconductors. For example, Annett *et al* [9] and Hirschfeld and Goldenfeld [10], have shown that the impurity scattering can convert the T -linear behavior of the low-temperature superfluid density to a T^2 behavior, in agreement with experiment. Other workers [11–13] have refined the theory so that it now agrees quite well with experiment. Choi [14] has used a t-matrix formalism to calculate the Zn impurity dependence of the superfluid density in $\text{YBa}_2\text{Cu}_3\text{O}_{7-\delta}$ for various temperatures. Salluzzo *et al* [15] used a model of dirty d-wave superconductivity to fit the impurity-dependence of the superfluid density in a NdBa-based cuprate superconductor. Hettler and Hirschfeld [16] have shown how inhomogeneities in a d-wave order parameter can lead to both strong suppression of superfluid density and enhanced microwave conductivity.

Several authors have treated the impurity problem by solving the Bogoliubov-de Gennes equations [1] for the pairing amplitude, which is position-dependent in a dirty d-wave or s-wave superconductor with a short coherence length. Ghosal *et al* [17] used this approach to show that disorder in a 2D s-wave superconductor reduces the effective superfluid density, makes the superfluid inhomogeneous, and even breaks up the 2D layer into superconducting islands. More recently [18], the same authors generalized this approach to d-wave superconductors. Zhitomirsky and Walker [19] showed how spatial fluctuations in the energy gap can reduce T_c in a d-wave superconductor. Haas *et al* [20] solved the Bogoliubov-de Gennes equations with a momentum-dependent pairing interaction to obtain an extended gapless region in the overdoped cuprates, which they connected to a rapid doping-induced decrease of both T_c and superfluid density. Franz *et al* [21], using the Bogoliubov-de Gennes approach for a spatially varying energy gap, found that the superfluid density goes rapidly to zero with increasing Zn concentration, while T_c decreases much more slowly with concentration, in reasonable agreement with experiment. Neto [22] has treated the Zn-doped cuprates as a collection of fluctuating stripes modeled as an array of coupled overdamped Josephson junctions pinned by impurities, and has used this model to estimate the doping-dependence of the transition temperature. Finally, Uemura [23] has discussed the low-temperature superfluid density in Zn-doped cuprates from the point of view of the “universal correlation” between T_c and zero-temperature superfluid density in the underdoped cuprates. As noted by Emery and Kivelson [24], such a connection would exist if T_c were controlled by phase fluctuations rather than by the vanishing of the gap amplitude.

Most of these models require a rather elaborate calculation to find the influence of nonmagnetic impurities on the superfluid density. By contrast, the goal of this paper is to analyze the behavior to be expected of a very simple model of the Zn-doped cuprate superconductors which can be worked out by intuitively appealing calculations. Although this model is difficult to derive from first principles, it may still be of value, because it can be used to make simple predictions for specific experiments, and to understand trends in those experiments.

The model we study was first described by Nachumi *et al* [25], and is sometimes known as the “Swiss cheese” model. In this model, the Zn atoms are assumed to replace the Cu atoms substitutionally within the CuO_2 layer, which is believed to be the locus of super-

conductivity in the cuprate superconductors, and to disrupt the $d_{x^2-y^2}$ order parameter, producing a region approximately of radius ξ_{ab} within which the layer is normal. (Here ξ_{ab} is the zero-temperature in-plane coherence length of $\text{YBa}_2\text{Cu}_3\text{O}_{7-\delta}$.) This disruption is plausible, because ξ_{ab} is very small in the cuprate superconductors (probably on the order of 10 - 20 Å at low temperatures, as discussed further below). Indeed, some dramatic experimental evidence supporting both the Swiss cheese model and the d-wave order parameter picture has recently been presented by Pan *et al* [26]. These workers showed, using scanning tunneling microscopy, that the gap was significantly suppressed near the Zn atoms, and that the density of states of single-particle excitations near the Zn atoms exhibited a fourfold symmetry.

In the present paper, we extend the approach of Nachumi *et al* by analyzing the Swiss cheese model within a simple percolation picture. Our approach differs from that of Nachumi *et al* by accounting for the connectivity of the superconducting part of the CuO_2 layer. By contrast, in their approach, the superfluid density is directly proportional to the superconducting area. The consequences of our approach are easily worked out if we use percolation theory and interpret the CuO_2 layer as an inhomogeneous superconductor with spatially distinct superconducting and normal region. The resulting variation of superfluid density with Zn concentration seems to agree somewhat better with experiment than does the simplest version of the Swiss-cheese model.

The remainder of this paper is organized as follows. In the next section, we describe our percolation model in detail. The numerical results following from this model are presented in Section III. Finally, in Section IV, we discuss our numerical results, briefly compare them to experiment, and analyze the limitations and predictions of the model.

II. MODEL

A. Geometrical Assumptions

Fig. 1 shows our picture of a single CuO_2 layer in Zn-doped $\text{YBa}_2\text{Cu}_3\text{O}_{7-\delta}$, in which a fraction x of the Cu atoms are replaced at random by Zn. Within the “Swiss cheese” model [25], each Zn atom completely suppresses superconductivity in a region of area $\pi\xi_{ab}^2$ around it. Thus, as x increases, a smaller and smaller areal fraction of the CuO_2 plane is superconducting. Eventually, for a large enough x , the remaining superconducting region is disconnected and the effective superfluid density must vanish.

There are two parameters in our geometrical model: the fraction x of in-plane Cu atoms which are replaced by Zn, and the quantity ξ_{ab}/a , which is the ratio of the zero-temperature in-plane coherence length ξ_{ab} (evaluated at $x = 0$) to the Cu-Cu distance a . Neither parameter is trivial to determine experimentally. For example, x is not necessarily equal to c , the *overall* fraction of Cu atoms which are replaced by Zn. In fact, it is believed that $x \sim 3c/2$, i. e., that all the Zn dopant atoms go into the CuO_2 planes [27]. Obviously, the connection between x and c is important in making quantitative comparisons between theory and experiment. Also, the magnitude of ξ_{ab} is not universally agreed upon for any value of δ . Nachumi *et al* [25], for example, quote $\xi_{ab} = 18.3\text{Å}$ at $c = 0$ and $\delta = 0.37$, extrapolating from $c = 0.01$. Since $a = 3.86\text{Å}$ for this value of δ [28], this gives $\xi_{ab}/a = 4.74$.

We shall later discuss the effects of assumptions about ξ_{ab} on the predictions obtained from this model.

B. Assumptions about σ_S and σ_N

To estimate the superfluid density as a function of x , we assume that the region more than a distance ξ_{ab} from any Zn atom has a complex conductivity $\sigma_S(\omega)$ characteristic of a superconductor. We obtain this conductivity by using the first London equation, as applied to a CuO_2 plane at $x = 0$:

$$\Lambda \frac{\partial \mathbf{J}_s}{\partial t} = \mathbf{E}, \quad (1)$$

where \mathbf{J}_s is the supercurrent density and \mathbf{E} is the electric field. In gaussian units,

$$\Lambda = \frac{4\pi\lambda_{ab}^2}{c^2} = \frac{m^*}{n_S q^2}, \quad (2)$$

where λ_{ab} is the in-plane penetration depth (evaluated at $x = 0$), and $m^* = 2m_e$ is the mass and $q = 2|e|$ the charge of a Cooper pair. Fourier transforming gives $\mathbf{J}_s(\omega) = \sigma_S(\omega)\mathbf{E}(\omega)$, where

$$\sigma_S(\omega) = \frac{iA}{\omega} \quad (3)$$

with

$$A = \frac{q^2 n_S}{m^*} = \frac{c^2}{4\pi\lambda_{ab}^2}. \quad (4)$$

We assume that the region *within* a distance ξ_{ab} of a Zn atom is simply a normal metal with frequency-independent conductivity σ_N .

Clearly, this simple model can only be appropriate for $\omega \ll \omega_0$, where $\omega_0 = A/\sigma_N$. At higher frequencies, there will be effects arising from the superconducting energy gap, which will produce additional structure in $\sigma_S(\omega)$. Also, this inductive form also implies no absorption at low frequencies in the limit $x \rightarrow 0$. In reality, many of the cuprate superconductors do exhibit low-frequency absorption, even at low temperatures [29]. This extra absorption can readily be included within the present model by adding to σ_S a parallel normal conductivity. We have carried out a few calculations including this extra term; as discussed below, they do not affect the x -dependent superfluid density.

C. Definition of Effective Superfluid Density $n_{S,e}(x)$

We may infer the effective superfluid density $n_{S,e}(x)$ from an effective London equation

$$\Lambda_e \frac{\partial \langle \mathbf{J} \rangle}{\partial t} = \langle \mathbf{E} \rangle \quad (5)$$

which relates the space-averaged current density $\langle \mathbf{J} \rangle$ to the space-averaged electric field $\langle \mathbf{E} \rangle$. $\Lambda_e(x)$ is related to $n_{S,e}(x)$ through a concentration-dependent generalization of eq. (2):

$$\Lambda_e(x) = \frac{4\pi}{\lambda_{ab,e}^2(x)} c^2 = \frac{m^*}{n_{S,e}(x) q^2}. \quad (6)$$

In the frequency domain, eqs. 5 and 6 may be written

$$\langle \mathbf{J}(\omega) \rangle = i \frac{n_{S,e} q^2}{m^* \omega} \langle \mathbf{E}(\omega) \rangle \equiv \sigma_e(\omega) \langle \mathbf{E}(\omega) \rangle, \quad (7)$$

where $\sigma_e(\omega, x)$ is the effective complex conductivity. Therefore,

$$n_{S,e}(x) = \frac{m^*}{q^2} \text{Lim}_{\omega \rightarrow 0} \omega \text{Im} \sigma_e(\omega, x), \quad (8)$$

and, in order to compute $n_{S,e}(x)$, we need to calculate $\sigma_e(\omega, x)$ at sufficiently low frequencies.

The ratio $n_{S,e}(x)/n_{S,e}(0)$ can also be calculated more directly by using a homogeneity property of σ_e [33]. In the present context, this property states that

$$\sigma_e(\sigma_S, \sigma_N, x) = \mu \sigma_e(\sigma_S/\mu, \sigma_N/\mu, x) \quad (9)$$

Here $\sigma_e(\sigma_S, \sigma_N, x)$ is the effective complex conductivity of a two-component system made up of constituents with conductivities σ_S and σ_N and in-plane Zn concentration x *in a particular geometry*, and μ is an arbitrary constant. In effect, homogeneity means that (for fixed geometry and fixed x) if the conductivities of each constituent are multiplied by a certain factor $1/\mu$, the *effective* conductivity is multiplied by that same factor $1/\mu$. In particular, if $\mu = \sigma_S$, we get

$$\sigma_e(\sigma_S, \sigma_N, x) = \sigma_S \sigma_e(1, \sigma_N/\sigma_S, x). \quad (10)$$

Hence, for any x ,

$$\frac{n_{S,e}(x)}{n_{S,e}(0)} = \frac{\text{Lim}_{\omega \rightarrow 0} \omega \text{Im} \sigma_e(\sigma_S(\omega), \sigma_N, x)}{\text{Lim}_{\omega \rightarrow 0} \omega \text{Im} \sigma_e(\sigma_S(\omega), \sigma_N, 0)} \quad (11)$$

$$= \frac{\sigma_e(1, 0, x)}{\sigma_e(1, 0, 0)}. \quad (12)$$

Here we have used the fact that $n_{S,e}(0)$, the superfluid density at $x = 0$, is given by $n_{S,e} = m^* A/q^2$, and also the fact that $\text{Lim}_{\omega \rightarrow 0} \sigma_N/\sigma_S(\omega) = 0$.

D. Two Methods for Calculating $n_{S,e}(x)$

We have evaluated $n_{S,e}(x)$ [or equivalently, $\sigma_e(\omega, x)$] by two complementary methods. The first method is a finite-element technique, and should become very accurate for a sufficiently large numerical sample, given the geometrical assumptions of the model. We consider an $L \times L$ region of a CuO_2 plane, assuming that the Cu ions sit on a square lattice of lattice

constant a , and choosing $L = N_x a$ where N_x is an integer. Then, using a random number generator, we replace a fraction x of the Cu ions by Zn. We then assign conductances $\sigma_S(\omega)$ or σ_N to each bond connecting nearest neighbor Cu sites, by the following rule. If the entire length of the bond is at least a distance ξ_{ab} from any Zn site, it is assigned a conductance $\sigma_S(\omega)$; otherwise, it is assigned σ_N . Next, we calculate $\sigma_e(\omega, x)$ using a standard technique known as the Y- Δ transformation [30], which is very efficient and accurate for two-dimensional impedance networks. This technique is approximate only insofar as it is limited to finite networks. We call this method the random conductance approach (RCA).

Our second method for calculating $\sigma_e(\omega, x)$ is a simple analytical approximation, the effective medium approximation (EMA) [31–33]. For the assumed geometry, this approximation is implemented as follows. First, we calculate p , the areal fraction occupied by the superconducting material, as a function of x , using the relation

$$p = \text{Lim}_{S \rightarrow \infty} \left(1 - \frac{\pi \xi_{ab}^2}{S} \right)^{N_{Zn}}, \quad (13)$$

where N_{Zn} is the number of Zn ions in a plane of area S . This limit is readily evaluated using the relation $x = N_{Zn} a^2 / S$, with the result

$$p = \exp \left(-x \frac{\pi \xi_{ab}^2}{a^2} \right). \quad (14)$$

Given p , one can calculate σ_e using the standard EMA relation for this two-dimensional system, namely,

$$p \frac{\sigma_N - \sigma_e}{\sigma_N + \sigma_e} + (1 - p) \frac{\sigma_S - \sigma_e}{\sigma_S + \sigma_e} = 0. \quad (15)$$

The physically correct solution to this quadratic equation is the one which satisfies $\text{Im} \sigma_e > 0$. Of course, ideally, the EMA is suited for application to a geometry in which the N and S components are distributed in a symmetrical fashion, whereas here, because of the assumption of excluded area, the N and S are not distributed symmetrically. Nonetheless, it is a reasonable approximation even for this nonsymmetric geometry.

Once $\sigma_e(\omega)$ has been calculated at a given x by either of the methods described above, the effective superfluid density can be inferred from the relation (8). We can also compute the ratio $n_{S,e}(x)/n_{S,e}(0)$ directly, using eq. (12). That is, for a given x , we decide which are the superconducting bonds, using the method described earlier in this section, and assign these bonds conductances of unity. The remaining normal bonds are assigned conductances of zero. The effective conductance is then evaluated using either the EMA or the RCA, and the ratio $n_{S,e}(x)/n_{S,e}(0)$ is then obtained using eq. (12).

III. RESULTS

In carrying out the RCA calculations, we have generally used a square networks of size ranging from 160×160 to 500×500 Cu sites. In order to reduce statistical fluctuations, the RCA results quoted below are averaged over a number of different realizations of the disorder for each ω and x . These realizations are “correlated” in the sense that, for each

realization, we increase x by adding a few impurities to the configuration of the previous x value. In evaluating the EMA conductivities, no such averaging is necessary, since the approximation can be evaluated analytically in the limit of a very large sample.

Our results for $n_{S,e}(x)/n_{S,e}(0)$ are shown in Fig. 2 for several choices of the parameter ξ_{ab}/a . The full, dashed, dot-dashed, and dotted curves are the EMA results. The diamonds are the results of the RCA calculations at $\xi_{ab}/a = 4.74$, using eq. (12), for two correlated realizations of a 500×500 lattice. There are several striking features. First of all, in both methods $n_{S,e}(x)/n_{S,e}(0)$ monotonically decreases with increasing x , reaching zero at a percolation threshold x_c which depends on ξ_{ab}/a . Moreover, x_c increases with decreasing ξ_{ab}/a . This relationship is not surprising: a larger ξ_{ab}/a implies that a larger area is converted from superconducting to normal by a single Zn impurity, within this model. Also, the EMA and RCA agree quite well over most of the concentration range, except near the percolation threshold. The EMA percolation threshold always corresponds to $p = 0.5$ [33]. The RCA threshold is higher, because the superconducting fraction remains connected to a somewhat higher fraction of Zn than is predicted by the EMA.

In Figs. 3 and 4, we show $\text{Im}\sigma_e(\omega, x)/\sigma_N$ and $\text{Re}\sigma_e(\omega, x)/\sigma_N$ as a function of x at $\omega = 0.001\omega_0$, where $\omega_0 = A/\sigma_N$ and A is defined in eq. (4). We use using parameters thought to be appropriate for the case $\delta = 0.37$, namely, $\xi_{ab}/a = 4.74$ [28]. In both Figures, the dashed line represents the EMA; the diamonds denote the RCA (average over 20 correlated realizations of a 160×160 lattice) and the the open squares are the RCA, averaged over 2 realizations of a 500×500 lattice. Fig. 3 shows that $\text{Im}\sigma_e(\omega, x)/\sigma_N$ closely mirrors the behavior of $n_{S,e}(x)/n_{S,e}(0)$ shown in Fig. 2, as expected from the homogeneity relations (11) and (12). The apparent percolation threshold is again somewhat larger ($x_c \sim 0.014$) in the RCA than in the EMA ($x_c \sim 0.01$). For values of x well below x_c , $\text{Im}\sigma_e(\omega = 0.001\omega_0, x)/\sigma_N$, like $n_{S,e}(x)/n_{S,e}(0)$, decreases linearly with x . This linear behavior is well known in the EMA [33].

Fig. 4 shows that $\text{Re}\sigma_e(\omega, x)$ has a strong peak occurring near the percolation threshold ($x_c \sim 0.01$ in the EMA and ~ 0.014 within the RCA for our choice of ξ_{ab}/a). The physical origin of this peak is discussed in the next section. We believe that the greater half-width of the RCA results arises because the calculation is carried out for a finite sample, and also because the average is taken over a number of different realizations, each of which has a slightly different percolation threshold for these finite samples. In support of this picture, note that the RCA half-width is smaller for the larger (500×500) samples, for which these fluctuations should be smaller. The slight random fluctuations in these curves as a function of x are, we believe, also due to these finite-size effects. By contrast, the EMA results are obtained analytically for an effectively infinite sample; so these finite-size fluctuations play no role. Note that, even for a 500×500 sample, there are still only 375 impurities at $x = 0.015$; so these fluctuations are still significant in the RCA.

In Fig. 5, we show $\text{Re}\sigma_e(\omega, x)/\sigma_N$ for $\omega = 0.0001\omega_0$, once again using $\xi_{ab}/a = 4.74$, as calculated in the EMA and in the RCA for two different sample sizes. The EMA peak is clearly stronger for $\omega = 0.0001\omega_0$ than $\omega = 0.001\omega_0$. The RCA peak is also stronger, especially for the larger sample where the peak height is not washed out by finite size effects. The apparent double peak for the 500×500 sample is, we believe, just the result of finite-size fluctuations, which are magnified at such low frequencies where the conductivity contrast $|\sigma_S/\sigma_N|$ is larger.

Finally, we have calculated $\sigma_e(\omega, x)/\sigma_N$ within the EMA for the same model as before, again with $\xi_{ab}/a = 4.74$, but a slightly different choice for $\sigma_S(\omega)$. Namely, we write

$$\sigma_S(\omega) = \frac{iA}{\omega} + \sigma'_N, \quad (16)$$

where we arbitrarily choose $\sigma'_N = \sigma_N$. The motivation behind this choice is that, in a material such as $\text{YBa}_2\text{Cu}_3\text{O}_{7-\delta}$, which is believed to have an order parameter with $d_{x^2-y^2}$ symmetry, the in-plane conductivity is expected to have a quasiparticle contribution, even at very low temperatures. The additional term σ'_N is a crude way of modeling this contribution. The resulting $\text{Re}\sigma_e(\omega, x)$ is plotted versus x at $\omega = 0.001\omega_0$, both for the model (16) and for a purely inductive $\sigma_S = iA/\omega$. Clearly, the peak near x_c is little affected by the change, but there is now, in addition, some extra contribution to $\text{Re}\sigma_e(\omega, x)$ for $x < x_c$. Although this extra contribution to σ_S does slightly change $\text{Re}\sigma_e(\omega, x)$ at finite ω , the homogeneity relations (11) and (12) imply that it has no effect on $n_{S,e}(x)$, either in the EMA or in the RCA.

IV. DISCUSSION

It is of interest to compare our calculated values of x_c with the experimentally observed critical concentration for $\text{YBa}_2(\text{Cu}_{1-c}\text{Zn}_c)_3\text{O}_{7-\delta}$ at $\delta = 0.37$. The critical value of c is between 0.02 and 0.03 [7,34–38] (probably closer to 0.03, judging from in-plane resistivity measurements [37]), as compared to our calculated critical value $x_c \sim 0.014$ for this δ [cf. Fig. 2]. But a direct comparison of these values is difficult: the in-plane Zn concentration may differ from c . If in fact $x \sim 3c/2$, as mentioned above, then our model seems to underestimate x_c ; the underestimate is less in the RCA than in the more approximate EMA. But this apparent discrepancy in x_c may not be very significant, for two reasons. First, x_c is quite sensitive to the parameter ξ_{ab}/a : a change of ξ_{ab} only from 4.74 to 3 increases x_c by more than a factor of 2 in the EMA, and presumably by a similar amount in the RCA. As already mentioned, this parameter is not known experimentally with great precision. Secondly, our model assumes that the CuO_2 layer undergoes an *discontinuous* change from S to N character at a distance ξ_{ab} from a Zn impurity. It would be more realistic to assume a gradual change. Although such a transition region might be difficult to include in the present model, its qualitative effect would probably be to reduce the effective radius of the normal region to a value smaller than ξ_{ab} . Such a reduction would, according to our results, *increase* x_c , making it closer to the reported value [37,38].

It is of interest to compare the present model to several others in the literature. In the original model of Nachumi *et al* [25], the superfluid density is proportional to the superconducting areal fraction, i. e., to the fraction of the CuO_2 plane which is more than a distance ξ_{ab} from any Zn impurity. The present model improves on the implementation of this Swiss cheese model by taking into account effects of connectivity of the superconducting parts. This treatment is consistent with the generalized London equation [eq. (5)]. In another class of models (see, e. g., Refs. [17,21]) $n_{S,e}(x)$ is calculated using the Bogoliubov-de Gennes equation with some form of static disorder. This model, like the Swiss-cheese model, also leads to a spatially varying gap function or pairing potential. Although this model seems quite different from ours, we speculate that both actually have much of the

same physical content. The difference is that in the models of Refs. [17,21], the disorder is on an atomic scale and treated microscopically, whereas in the present case the disorder is on a greater length scale and treated within continuum electrodynamics. Nonetheless, both lead to surprisingly similar behavior (superfluid density diminishing rapidly with increasing x and vanishing at a critical concentration). We do not know how to connect the two on a more rigorous basis, however.

A nontrivial prediction of the present model is the existence of a peak in $\text{Re}\sigma_e(\omega)$ near x_c . If such a peak were observed in experiments, it could be viewed as strong evidence in favor of the present model. This ‘‘percolation peak’’ is reminiscent of the well-known fluctuation peak in $\text{Re}\sigma(\omega)$ near T_c in a homogeneous superconductor, but there are significant differences in the underlying physics. The fluctuation peak results from slow motions of superconducting fluctuations with size of order $\xi_{ab}(T)$. The spatial extent of these fluctuations diverges near T_c , as does the time scale on which they move; this diverging time scale leads to a strong low-frequency peak in the conductivity. By contrast the percolation peak involves motion of charge carriers through a *static* disordered structure; the frequency-dependence arises from the slow motion of these charges through the weakly connected structure (but *static* structure of superconductor that exists, in our model, near the p_c (or x_c). The characteristic length for this structure is the so-called percolation correlation length ξ_p , which diverges near p_c on both sides of the percolation transition [33].

The existence of this percolation peak can be understood from the following crude argument. On the normal metal side of the percolation threshold, the static d. c. conductivity is finite, but should diverge as $p \rightarrow p_c$. This divergence is due to the ever-larger superconducting regions, which come closer and closer to shorting out the voltage across the normal metal as p_c is approached. This divergence should disappear as the frequency is increased, because the contrast in conductivities between superconducting and normal regions will become much smaller in absolute value (that is, the ratio $|\sigma_N/\sigma_S|$ should approach unity). Therefore, at a fixed p just above p_c (that is, on the normal metal side), $\text{Re}\sigma_e(\omega, p)$, should show a strong maximum at $\omega = 0$, and this maximum should diverge as $p \rightarrow p_c$. Since $\sigma_e(\omega, p)$ should vary continuously across the percolation threshold, except at exactly $\omega = 0$, we expect the same behavior on the superconducting side of the threshold. This is qualitatively the behavior we see in both our EMA and RCA results.

The behavior of this ‘‘critical peak’’ can be estimated from the standard scaling theory of the percolation threshold (see, for example, Ref. [33]). This scaling approach is based on the assumption that the percolation threshold is a critical point described by a single diverging length ξ_p ; if that assumption is correct, then the scaling approach is believed to be exact. As applied to the present model, and using the homogeneity relations (11) and (12), this scaling approach dictates that σ_e have the form

$$\sigma_e(1, \sigma_N/\sigma_S, x) = \sigma_S |\Delta x|^t F\left(\frac{\sigma_N/\sigma_S}{|\Delta x|^{s+t}}\right), \quad (17)$$

where $\Delta x = x - x_c$, and s and t are standard percolation exponents. The function $F(z)$ of the complex variable z has the limiting behaviors [33]

$$F(z) \sim C_1 z, |z| \ll 1; \Delta x > 0; \quad (18)$$

$$F(z) \sim C_2, |z| \ll 1; \Delta x < 0; \quad (19)$$

$$F(z) \sim C_3 z^{t/(t+s)}, |z| \gg 1, \quad (20)$$

where C_1 , C_2 , and C_3 are constants. This form implies that precisely at $x = x_c$ both the real and imaginary parts of σ_e satisfy

$$\text{Re}\sigma_e(\omega, x_c), \text{Im}\sigma_e(\omega, x_c) \propto \sigma_S^{s/(t+s)} \sigma_N^{t/(t+s)} \propto \omega^{-s/(t+s)}. \quad (21)$$

In conventional 2D percolation theory, $s = t \sim 1.30$; so both $\text{Re}\sigma_e(\omega, x_c)$ and $\text{Im}\sigma_e(\omega, x_c)$ would be proportional to $\omega^{-1/2}$. The present ‘‘Swiss cheese’’ model may not, however, be in the same universality class as percolation on a lattice. Instead, it may fall into the class of certain continuum percolation models [39]. In the present case, the exponent t and s should have the values corresponding to another ‘‘Swiss cheese’’ model in 2D, in which the area between the holes is conducting while the holes are insulating. According to the discussion of Ref. [39], the Swiss cheese t and s are, in fact, unchanged from their lattice values of 1.3 in two dimensions. Therefore, one still expects that both $\text{Re}\sigma_e(\omega, x_c)$ and $\text{Im}\sigma_e(\omega, x_c)$ should have a $\omega^{-1/2}$ frequency dependence in this model.

It is also of interest to consider the predictions of the present model regarding the *critical current density* $J_c(x)$ in Zn-doped $\text{YBa}_2\text{Cu}_3\text{O}_{7-\delta}$. In this case, we use the results of continuum percolation theory as applied to $J_c(x)$ [40], or equivalently, to $J_c(p)$. In two dimensions, for the present Swiss-cheese model, it is found [40] that $J_c(p) \propto (p - p_c)^\nu$. The critical exponent ν is estimated as $\nu = (\nu + 1)(d - 1)$ for Swiss cheese in d dimensions, where ν is the percolation correlation length exponent defined by $\xi_p \propto |p - p_c|^{-\nu}$. Thus, in two dimensions $\nu = \nu + 1$. The conductivity exponent t is unchanged from its lattice value in $d = 2$. Using the approximations $t \sim \nu = 4/3$ in $d = 2$ [41], we obtain $\nu \sim 7t/4$. Equivalently, this may be written (for p near the percolation threshold) $J_c(p)/J_c(1) \sim [n_{S,e}(p)/n_S]^{7/4}$. In terms of x , $J_c(x)/J_c(0) \propto [n_{S,e}(x)/n_{S,e}(0)]^{7/4}$. In summary, $J_c(x)$ in Zn-doped $\text{YBa}_2\text{Cu}_3\text{O}_{7-\delta}$ is predicted to go to zero near the percolation threshold even more rapidly than does $n_{S,e}(x)$. It would be of interest if this prediction could be tested experimentally.

The present model does not give any information directly about the superconducting transition temperature $T_c(x)$. Some experiments on Zn-doped $\text{YBa}_2\text{Cu}_3\text{O}_{7-\delta}$ indicate that $T_c(x)$ decreases much more slowly with x than does $n_{S,e}(x, T = 0)$ (see, for example, Ref. [7]). Although we have no quantitative model for this behavior, a simple qualitative argument does suggest an explanation. Let us suppose that $x < x_c$, so that the superconducting portion of the material is connected throughout the plane. In that case, if *thermal fluctuation effects* can be neglected, then $T_c(x)$ (as measured by a vanishing d. c. resistivity) should be *independent* of x for $x < x_c$, and zero for $x > x_c$. In this limit, clearly $T_c(x)/T_c(0) > n_{S,e}(x)/n_{S,e}(0)$. In reality, thermal fluctuations should reduce $T_c(x)$ below its expected value in the absence of fluctuations, but this inequality should still hold, as observed experimentally.

In summary, we have presented a simple model for the variation of superfluid density with in-plane Zn concentration x in Zn-doped $\text{YBa}_2\text{Cu}_3\text{O}_{7-\delta}$. The model is based on the ‘‘Swiss cheese’’ picture suggested by Nachumi *et al* [25]. Using this model, we calculate the ratio $n_{S,e}(x)/n_{S,e}(0)$ for Zn-doped $\text{YBa}_2\text{Cu}_3\text{O}_{7-\delta}$ as a function of the ratio ξ_{ab}/a , using two different approximations. The model predicts a critical Zn concentration above which $n_{S,e}(x)$ is zero, in rough agreement with experiment for Zn-doped $\text{YBa}_2\text{Cu}_3\text{O}_{7-\delta}$ at $\delta = 0.37$. The model also predicts a low-frequency peak in $\text{Re}\sigma_e(\omega)$ near x_c , the existence of which has apparently not been checked experimentally. Finally, the model suggests that

the low-temperature critical current ratio $J_c(x)/J_c(0) \sim [n_{S,e}(x)/n_{S,e}(0)]^{7/4}$ near $x = x_c$. The observation of these features would give additional experimental support to the present simple model.

V. ACKNOWLEDGEMENTS

We would like to thank Professor Thomas R. Lemberger for helpful discussions. Jeng-Da Chai thanks L. J. Schradin for valuable discussions regarding computation and M. E. Howard for useful comments on the manuscript. This work has been supported by NSF Grant No. DMR97-31511.

REFERENCES

- [1] For a discussion, see, e. g., M. Tinkham, “Introduction to Superconductivity,” 2nd Edition (McGraw-Hill, New York, 1996), pp. 386-87.
- [2] D. A. Wollman, D. J. Van Harlingen, W. C. Lee, D. M. Ginsberg, and A. J. Leggett, Phys. Rev. Lett. **71**, 2134 (1993); C. C. Tsuei, J. R. Kirtley, C. C. Chi, L. S. Yujahnes, A. Gupta, T. Shaw, J. Z. Sun, and M. B. Ketchen, Phys. Rev. Lett. **73**, 593 (1994).
- [3] E. R. Ulm, J.-T. Kim, T. R. Lemberger, S. R. Foltyn, and X. Wu, Phys. Rev. **B51**, 9193 (1995).
- [4] J. Jung, B. Boyce, H. Yan, M. Abdelhadi, J. Skinta, T. R. Lemberger, J. Superconductivity **13**, 753 (2000).
- [5] K. Karpinska, M. Z. Cieplak, S. Guha, A. Malinowski, T. Skoskiewicz, W. Pelsiewicz, M. Berkowski, B. Boyce, T. R. Lemberger, and P. Lindenfeld, Phys. Rev. Lett. **84**, 155 (2000).
- [6] D. N. Basov, A. V. Puchkov, R. A. Hughes, T. Strach, J. Preston, T. Timusk, D. A. Bonn, R. Liang, and W. N. Hardy, Phys. Rev. **B49**, 12165 (1994).
- [7] C. Bernhard, J. L. Tallon, C. Bucci, R. DeRenzi, G. Guidi, G. V. M. Williams, and C. Niedermeyer, Phys. Rev. Lett. **77**, 2304 (1996).
- [8] S. H. Moffat, R. A. Hughes, and J. S. Preston, Phys. Rev. **B55**, 14741 (1997).
- [9] J. F. Annett, N. D. Goldenfeld, and S. R. Renn, Phys. Rev. **B43**, 2778 (1991).
- [10] P. J. Hirschfeld and N. D. Goldenfeld, Phys. Rev. **B48**, 4219 (1993).
- [11] M. Prohammer and J. P. Carbotte, Phys. Rev. **B43**, 5370 (1991).
- [12] H. Kim, G. Preosti, and P. Muzikar, Phys. Rev. **B49**, 3544 (1994).
- [13] Y. Sun and K. Maki, Phys. Rev. **B51**, 9193 (1995).
- [14] C. H. Choi, J. Korean Physical Society **37**, 552 (2000),
- [15] M. Salluzzo, F. Palomba, G. Pica, A. Andreone, I. Maggio-Aprile, O. Fischer, C. Cantoni, D. P. Norton, Phys. Rev. Lett. **85**, 1116 (2000).
- [16] M. H. Hettler and P. J. Hirschfeld, Phys. Rev. **B59**, 9606 (1999).
- [17] A. Ghosal, M. Randeria, and N. Trivedi, Phys. Rev. Lett. **81**, 3940 (1998).
- [18] A. Ghosal, M. Randeria, N. Trivedi, Phys. Rev. **B630505** (2001).
- [19] M. E. Zhitomirsky and M. B. Walker, Phys. Rev. Lett. **80**, 5413 (1998)
- [20] S. Haas, A. V. Balatsky, M. Sigrist, and T. M. Rice, Phys. Rev. **B56**, 5108 (1997).
- [21] M. Franz, C. Kallin, A. J. Berlinsky, and M. I. Salkola, Phys. Rev. **B56**, 7882 (1997).
- [22] A. H. C. Neto, Phys. Rev. Lett. **87**, 3931 (1997).
- [23] Y. J. Uemura, Physica C **341**, 2117 (2000); Int. J. Mod. Phys. B **14**, 3713 (2000).
- [24] V. Emery and S. A. Kivelson, Nature **374**, 434 (1995).
- [25] B. Nachumi, A. Keren, K. Kojima, M. Larkin, G. M. Luke, J. Merrin, O. Tchernyshov, Y. J. Uemura, N. Ichikawa, M. Goto, and S. Uchida, Phys. Rev. Lett. **77**, 5421 (1996).
- [26] S. H. Pan, E. W. Hudson, K. M. Lang, H. Eisaki, S. Uchida, and J. C. Davis, Nature **403**, 746 (2000),
- [27] R. P. Gupta and M. Gupta, Phys. Rev. **59**, 3381 (1999).
- [28] K. Kakurai, S. Shamoto, T. Kiyokura, M. Sato, J. M. Tranquada, and G. Shirane, Phys. Rev. **B48**, 3485 (1993).
- [29] See, for example, J. Corson, J. Orenstein, S. Oh, J. O’Donnell, and J. N. Eckstein, Phys. Rev. Lett. **85**, 2569 (2000).
- [30] D. J. Frank and C. J. Lobb, Phys. Rev. **B37**, 302 (1988).

- [31] D. A. G. Bruggeman, *Ann. Physik (Leipzig)* **24**, 636 (1935).
- [32] R. Landauer, *J. Appl. Phys.* **23**, 779 (1952).
- [33] D.J. Bergman and D. Stroud, *Solid State Phys.* **46**, 147 (1992).
- [34] Grzegorz Haran and A. D. S. Nagi, *Phys. Rev.* **B58**, 12441 (1998).
- [35] T. Xiang and J. M. Wheatley, *Phys. Rev.* **B51**, 11721 (1995).
- [36] B. Jayaram, S. K. Agarwal, C. V. Narasimha Rao, and A. V. Narlikar, *Phys. Rev.* **B38**, 2903 (1988).
- [37] K. Mizuhashi, K. Takenaka, Y. Fukuzumi, and S. Uchida, *Phys. Rev.* **B52**, 3884 (1995).
- [38] L. Raffo, F. Licci, and A. Migliori, *Phys. Rev.* **B48**, 1192 (1993).
- [39] S. Feng, B. I. Halperin, and P. N. Sen, *Phys. Rev.* **B35**, 197 (1987).
- [40] C. J. Lobb, P. M. Hui, and D. Stroud, *Phys. Rev.* **36**, 1956 (1987).
- [41] C. J. Lobb and K. R. Karasek, *Phys. Rev.* **B25**, 492 (1982) and references cited therein.

FIGURES

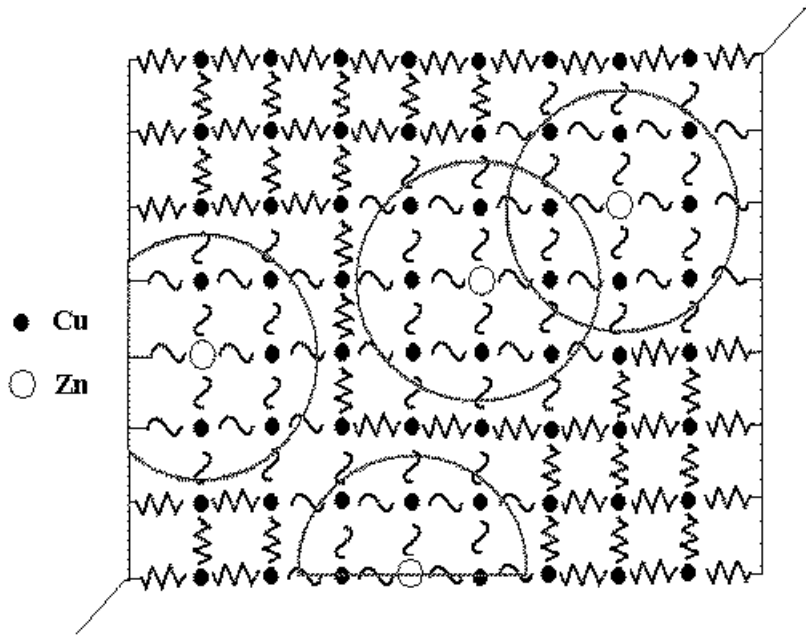


FIG. 1. Schematic diagram of model used to calculate effective superfluid density of Zn-doped $\text{YBa}_2\text{Cu}_3\text{O}_{7-\delta}$. Shown is a sketch of a section of a CuO_2 plane. The filled circles represent Cu ions. The open circles represent Zn ions, which have substitutionally replaced the Cu ions. O ions (not shown) are situated in the middle of each bond. The resistor-like and wavy lines represent superconducting and normal bonds in our model. The large circles, of radius ξ_{ab} , represent the regions which are assumed to have been driven normal by the Zn ions. The two diagonal lines represent the leads used in the application of the Y- Δ transformation.

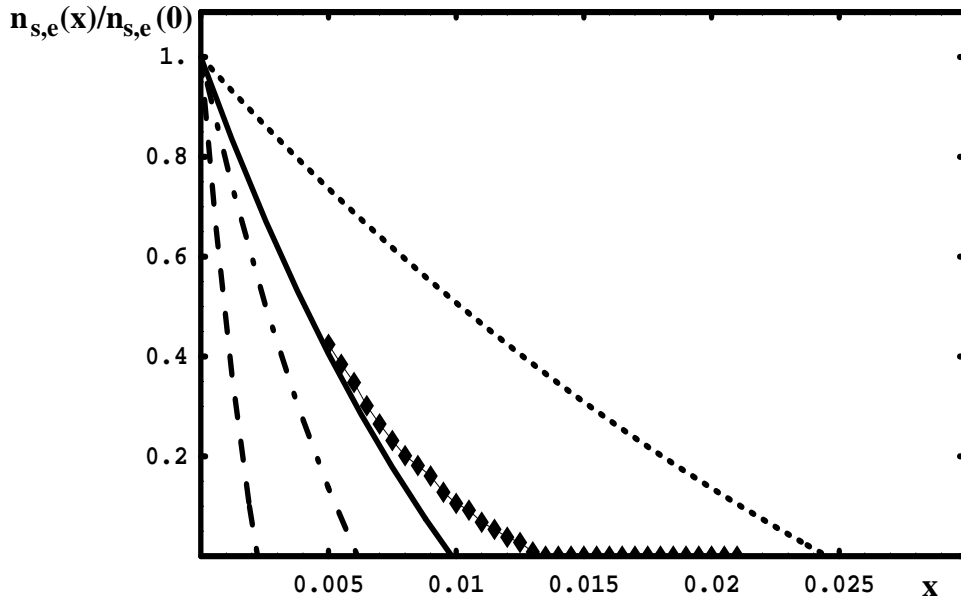


FIG. 2. Relative zero-temperature superfluid density $n_{S,e}(x)/n_{S,e}(0)$, plotted as a function of in-plane Zn atomic concentration x for various values of the ratio ξ_{ab}/a , where ξ_{ab} is the zero-temperature in-plane coherence length and a the lattice constant (Cu-Cu spacing). Dotted, solid, dot-dashed and dashed curves correspond to EMA calculations carried out within the “Swiss cheese” model as described in the text, for $\xi_{ab}/a = 3, 4.74, 6$ and 10 respectively. Filled diamond symbols are results for $\xi_{ab}/a = 4.74$ but calculated in the RCA. Line segments connecting the diamonds are guides to the eye. Note the difference in the percolation threshold: x_c is greater for the RCA than for the EMA.

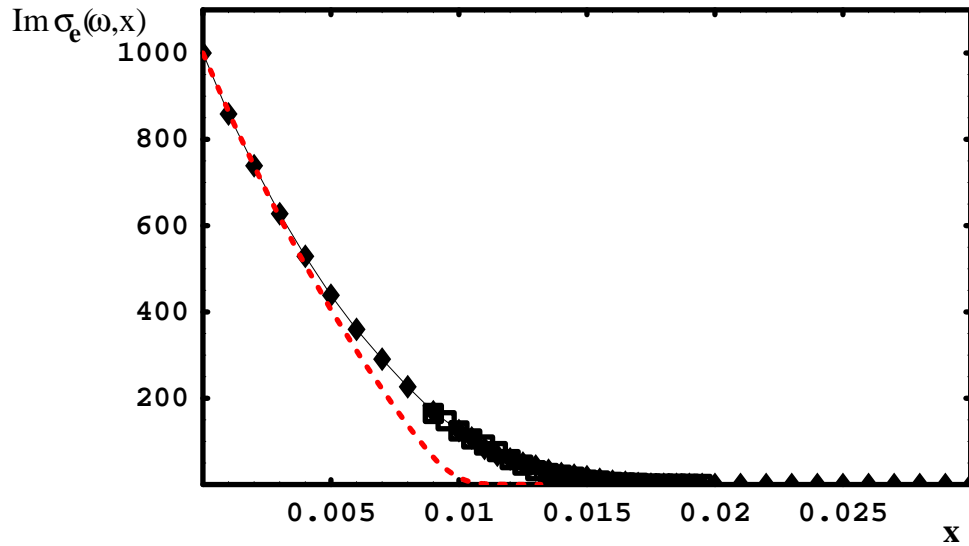


FIG. 3. $\text{Im}\sigma_e(\omega, x)/\sigma_N$ versus in-plane Zn atomic concentration x for $\omega = 0.001\omega_0$, where $\omega_0 = A/\sigma_N$, assuming $\xi_{ab}/a = 4.74$. We use $\sigma_S(\omega) = iA/\omega$, $\sigma_N = \text{const}$. Filled diamonds are RCA calculations for a 160×160 lattice, averaged over twenty correlated realizations; open squares are RCA for two correlated realizations of a 500×500 lattice). Solid line through these points is a guide to the eye. Dashed line: effective-medium approximation (EMA).

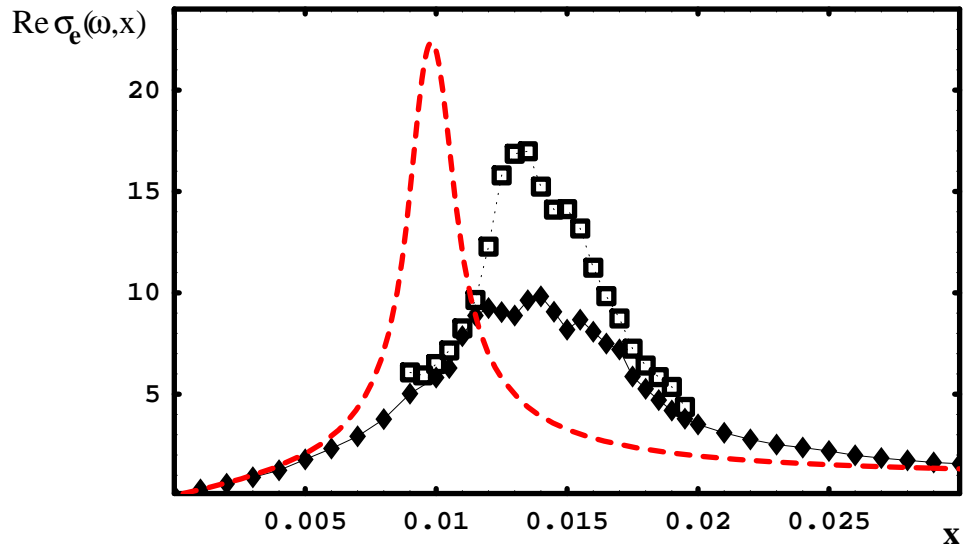


FIG. 4. Same as Fig. 3 but for $\text{Re}\sigma_e(\omega, x)/\sigma_N$. Solid and dotted lines are guides to the eye. The RCA calculations for the larger size are carried out only between $x = 0.0095$ and $x = 0.02$.

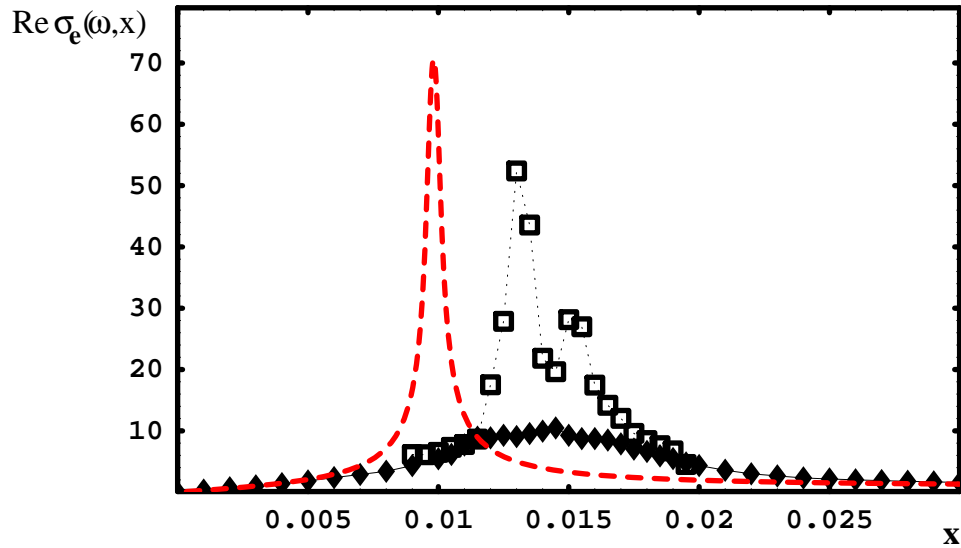


FIG. 5. Same as Fig. 4 but for $\omega = 0.0001\omega_0$, $\xi_{ab}/a = 4.74$. In this case, the full diamonds represent twenty correlated realizations of the RCA for a 140×140 lattice, and the open squares are two realizations for a lattice of size 500×500 . This latter calculation is carried out only between $x = 0.01$ and $x = 0.02$. Light solid and dotted lines just connect the calculated points. Dashed line with no data points: EMA.

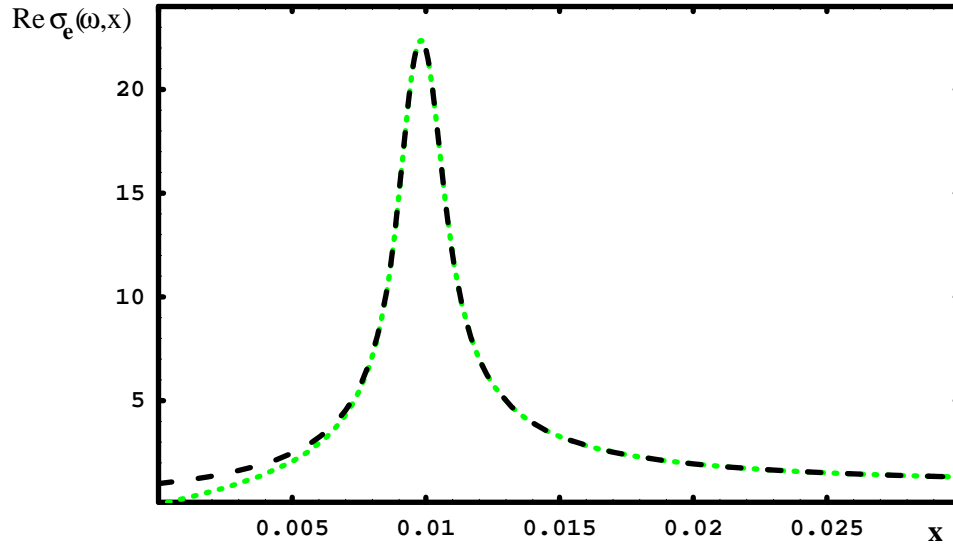


FIG. 6. $\text{Re}\sigma_e(\omega, x)/\sigma_N$ as calculated in the EMA for two cases. Dotted curve: $\sigma_S(\omega) = iA/\omega$, $\sigma_N = \text{const.}$; dashed curve: $\sigma_S(\omega) = iA/\omega + \sigma_N$, $\sigma_N = \text{const.}$ Units are same as in Figs. 2-5.